JOURNAL OF CHEMICAL INFORMATION AND MODELING

Article

pubs.acs.org/jcim

Integration of Ligand Field Molecular Mechanics in Tinker

Marco Foscato,[†] Robert J. Deeth,*[,‡] and Vidar R. Jensen*[,†]

[†]Department of Chemistry, University of Bergen, Allégaten 41, N-5007 Bergen, Norway

[‡]Inorganic Computational Chemistry Group, Department of Chemistry, University of Warwick, Gibbet Hill Road, Coventry CV4 7AL, Great Britain

Supporting Information

ABSTRACT: The ligand field molecular mechanics (LFMM) method for transition-metal complexes has been integrated in Tinker, an easily available and popular molecular modeling software package. The capability to calculate LFMM potentials has been provided by extending the functional forms of the Tinker package as well as by integrating routines for calculating the ligand field stabilization energy (LFSE), which is central to LFMM. The capabilities of the implementation are illustrated by both static calculations on the two spin states of $[Fe(NH_3)_6]^{2+}$ and on $[Cu(NH_3)_m]^{2+}$ (m = 4, 5, 6) and dynamic (LFMD) simulations of an FeN_6-type spin-crossover compound. In addition to showing that results obtained with the Tinker-LFMM implementation are consistent with those of experiment and other computational methods and programs, we note that whereas LFMM is able to handle the conventional tetragonal Jahn−Teller distortion of the bond distances in $[Cu(NH_3)_6]^{2+}$, the LFSE term is also necessary in order to obtain even qualitatively correct coordination geometries for the two lower-coordinate copper complexes.

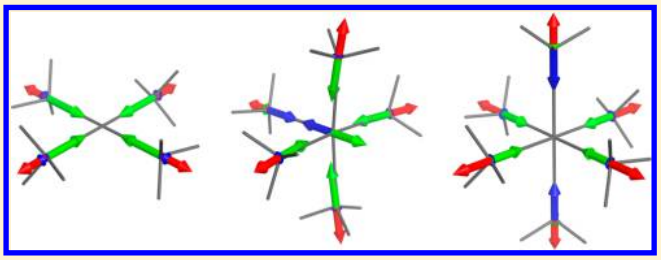

INTRODUCTION

Even though quantum-chemical methods, in particular density functional theory (DFT), are attractive in many areas of molecular modeling, the computational cost of such methods still hampers their application to large systems and cases where the potential needs to be generated quickly, such as in molecular dynamics (MD) and Monte Carlo (MC) simulations. Empirical force field-based molecular mechanics (MM) is an attractive alternative that has shown excellent performance in terms of efficiency and accuracy in applications for which suitable functional forms and force field parameters have been developed.[1,2] Whereas general and transferable force fields are available for vast ranges of chemical groups commonly found in organic compounds (e.g., MM3,[3] MMFF)[4] and biopolymers (e.g., AMBER),[5] the geometric (i.e., coordination numbers and geometries) and electronic (i.e., oxidation and spin states) flexibility characterizing transition-metal complexes still represents a major challenge for MM methods.[6]

To meet this challenge, dedicated force fields have been developed, either using the formalism of regular organic chemistry force fields or with additional terms accounting for the peculiarities of the metal sites.[7−11] Although numerous applications have shown that, with enough attention paid to parametrization, it is indeed possible to describe inorganic compounds using functional forms of regular organic chemistry force fields,[10−14] this approach lacks generality. For example, modeling of different electronic spin states may require significant adaptation of the force field and demanding reparametrizations.[9,11] In addition, truly broadly applicable sets of parameters, i.e., as in the universal force field,[15] are in general considerably less accurate than the regular organic chemistry force fields, and unfortunately, their accuracy is also insufficient for many applications.[6,16]

The main idea behind the alternative approaches has been to add supplementary terms in order to describe the particular requirements of the metal centers.[17,18] For example, angular bending terms around metal atoms have been based on models such as "points on a sphere" (POS), which conceptually is analogous to the valence shell electron pair repulsion (VSEPR) model and is implemented, for instance, in the MOMEC software,[7,19] or on the basic principles of valence bond theory, as implemented in both the SHAPES[18] and VALBOND[20−22] methods. Notably, the applications of valence bond theory and extensions thereof[23,24] have proved to reduce the parametrization problem and to need fewer parameters than do other force fields that use standard angle bending terms.[23]

Deeth and co-workers have exploited ligand field theory to derive an additional term that accounts for the ligand field stabilization energy (LFSE), thus providing a way to represent the stereoelectronic effects of partially filled d orbitals of transition-metal complexes.[25] This strategy has been implemented in the ligand field molecular mechanics (LFMM) method for Werner-type metal complexes.[25] Applications of this method have been reported for many of the first-row transition metals[26] and for Pt and Ru,[27,28] and it has been shown to be able to handle the Jahn−Teller effect,[29] the trans influence,[30] and even π bonding in transition-metal complexes.[28,31] The terms particular to LFMM are centered on the metal while standard implementations of organic chemistry

Received: February 20, 2015
Published: May 13, 2015

DOI: 10.1021/acs.jcim.5b00098
J. Chem. Inf. Model. 2015, 55, 1282−1290

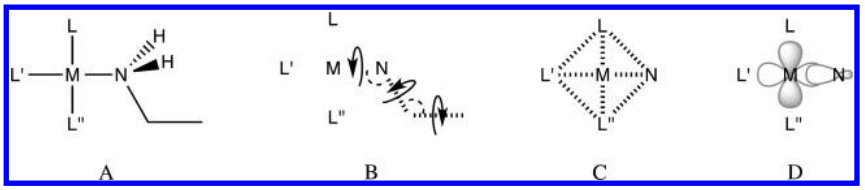

Figure 1. Schematic representation of the LFMM model for a simplified molecular structure (A): standard MM terms (B), MM-style terms introduced by LFMM (C), and AOM term (D). Stretching terms are depicted as hashed bonds, angle bending terms with dashed arches, and torsions with circular arrows. Hydrogen atoms, electron pairing terms, and nonbonded terms have been omitted for clarity.

force fields describe the organic portion of the complex (i.e., the organic ligands).[25,29,32,33] Thus, LFMM can be described as a hybrid method combining two empirical partners.[34,35] While this feature allows the use of standard organic chemistry force fields for the organic portion of the system, the LFMM terms require specific capabilities not available in common MM tools. Thus, LFMM has been implemented in relatively few molecular modeling software packages to date.

Deeth and co-workers integrated their LFMM code into the commercial software Molecular Operating Environment (MOE) to give the main and most frequently used implementation of LFMM, termed DommiMOE.[36,37] Apart from the very first implementation of LFMM, termed DOMMINO,[32] which was largely abandoned with the advent of DommiMOE because of the tedious preparation of input files and lack of parameters for the organic force field,[36] and an integration of LFMM within the package DL_POLY2,[38] which still depends on DommiMOE for the preparation of input files, other tools for the application of LFMM are not available. Another implementation of the method is known to be under development, however,[19] and alternative approaches requiring specific force field parameters have also been reported in the literature.[39−42] In particular, a ligand field model similar to that of Deeth has been used in combination with the polarizable force field AMOEBA, but this approach is not compatible with existing LFMM parametrizations.[42]

Broader availability of LFMM could open up a range of new and interesting applications to large systems, various computer simulation techniques, and large-scale design studies. Therefore, in an attempt to fill the gap between currently available LFMM implementations and the wish for more accessible tools,[23,34,43] we have integrated the LFMM method into Tinker,[44] a popular and readily available molecular modeling package. Although not formally open source, the Tinker source code can be obtained free of charge under a license agreement allowing for further development in the scientific community, which is not the case for the DommiMOE implementation. Thus, by preparing the routines needed for Tinker to support LFMM, we aim to increase the accessibility of the LFMM method and to spur a wider range of applications and efforts to develop new parameter sets.

THE LFMM MODEL

The LFMM model combines standard force field terms and LFMM terms concentrated on the metal centers. The standard force field treatment accounts for all of the interactions in the organic portion of a transition-metal complex as well as all of the nonbonded interactions and the torsional terms including the metal center. Standard stretching and bending terms involving the metal atoms are replaced by LFMM terms (eq 1; M = metal, L = ligand).

$$E_{\mathrm{tot}} = \sum_{\text{not ML}} E_{\mathrm{str}} + \sum_{\text{not LML}} E_{\mathrm{bend}} + \sum E_{\mathrm{tor}} + \sum E_{\mathrm{nb}} + \sum_{\text{metals}} E_{\mathrm{LFMM}} \quad (1)$$

The LFMM terms involve four kinds of contributions (eq 2): metal−ligand bond stretches (E_{ML}), ligand−ligand 1−3 interactions (E_{LL}), an electron pairing contribution (E_{pair}), and the LFSE. While the first two contributions, although independent from the standard force field adopted in the organic portion of the system, still adhere to conventional MM formalisms (i.e., harmonic, Morse, and Lennard-Jones potentials), the empirical estimation of the electron pairing energy (the two-electron part of the LFSE) essentially is a function of the metal−ligand bond length (see below), and the angular overlap model (AOM)[45] accounts for the one-electron contribution to the ligand field stabilization term (Figure 1).

$$E_{\mathrm{LFMM}} = E_{\mathrm{ML}} + E_{\mathrm{LL}} + E_{\mathrm{pair}} + \mathrm{LFSE} \quad (2)$$

The AOM is based on a simplified treatment of the molecular orbitals involved in the metal−ligand interaction.[29,46,47] While the AOM has been used extensively for the derivation and interpretation of spectroscopic properties,[48−51] in LFMM it represents the perturbation adopted to account for geometrical consequences of the stereoelectronic effects of the d electrons.[25] To this end, the ligand field potential is described as a sum of individual, local M−L contributions, each resolved into σ and π parts (mutually perpendicular π_x and π_y). For each M−L contribution, the angular dependence is related to the overlap of a metal d orbital with the ligand orbitals of proper symmetry. The strength of this interaction, which is the local contribution to the destabilization of the d orbitals, is modulated by the radial dependence according to the set of AOM parameters characterizing the given M−L pair and the given bond symmetry (σ, π_x, and π_y).[32]

Thanks to the local nature of the M−L contributions, the AOM approach does not require a priori assumptions about the coordination symmetry or the numbers and kinds of ligands. The empirical parameters adopted thus pertain to the identity of the metal and the ligand in a single M−L pair.[28] In addition to the σ and π parameters, which monitor the local σ and π bonding interactions, the AOM can also include secondary terms due to d−s mixing. The effect of d−s mixing parameters, e_{ds}, is symmetry-dependent, and provided that the symmetry dictates that the metal d_{z^2} and valence s orbitals transform as the same irreducible representation, it leads to a depression of the d_{z^2} orbital and a concomitant change in the LFSE. The latter depends on the symmetry, d configuration, and spin state and is best known for square-planar systems such as planar $[CuCl_4]^{2-}$, where the d_{z^2} orbital is ∼6000 cm^{-1} lower than computed in the absence of d−s mixing.

DOI: 10.1021/acs.jcim.5b00098
J. Chem. Inf. Model. 2015, 55, 1282−1290

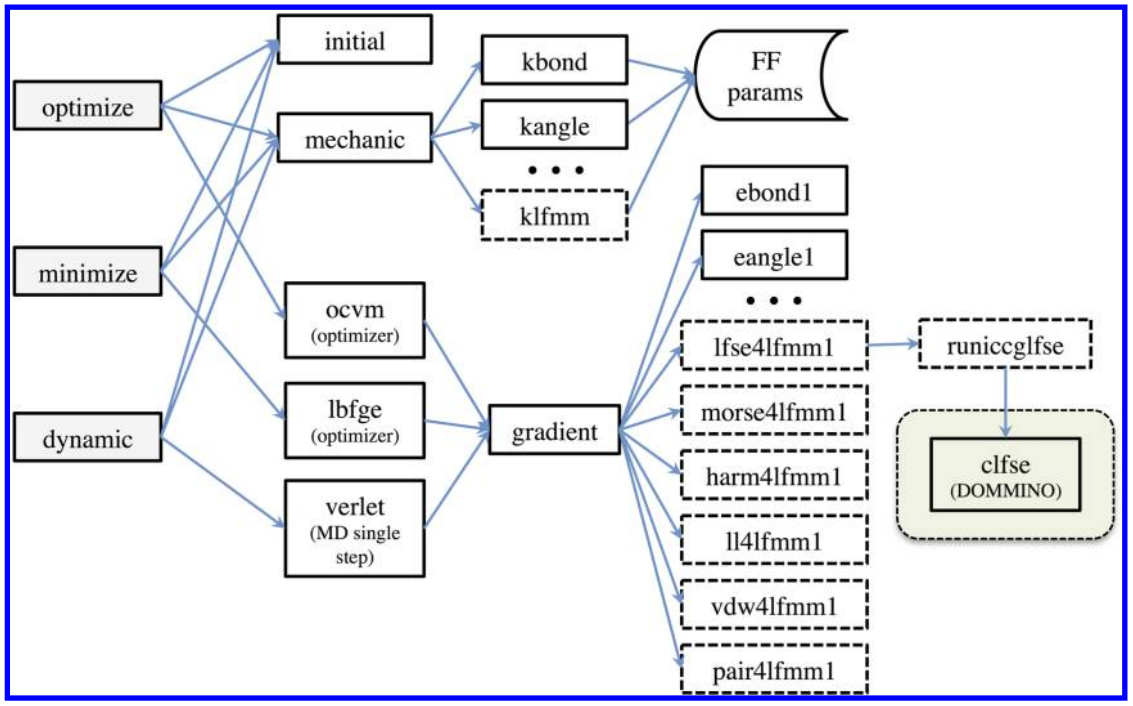

Figure 2. Simplified call graph for the Tinker programs *optimize*, *minimize*, and *dynamic*. Gray and white boxes are used for programs and subroutines, respectively. Dashed boxes represent the major extensions to the Tinker code related to the calculation of the energy and its gradient. The green box encapsulates all code deriving from the original implementation of LFMM.[32]

Although the same set of AOM parameters is often applied for different complexes containing the same M−L pair,[29,36] the transferability of the AOM parameters is not implicit in the AOM model.[48,52−54]

The AOM estimation of the LFSE results from the combination of the occupation numbers n_i of the d orbitals with the accompanying orbital energies ε_i (eq 3), which are obtained from diagonalization of the ligand field matrix $\mathbf{V}_{LF}$.[32]

$$\mathrm{LFSE} = \sum_i n_i \varepsilon_i \tag{3}$$

The elements of $\mathbf{V}_{LF}$ (eq 4) derive from the angular dependence $\mathbf{F}$, which accounts for the overlap of the d orbitals with ligand orbitals of proper symmetry (σ, π_x, or π_y), and the radial dependence factors e_k, which in turn are calculated from the M−L bond length (r_{ML}) and the set of AOM parameters ($a_{n,k,ML}$) for the given M−L pair (eq 5).

$$\langle d_i | V_{LF,ij} | d_j \rangle = \sum_{l}^{\text{ligands}} \sum_{k}^{\sigma,\pi_x,\pi_y} \mathbf{F}^*_{ik,l} \mathbf{F}_{kj,l} e_{k,l} \tag{4}$$

$$e_k = a_{0,k,\mathrm{ML}} + a_{1,k,\mathrm{ML}} r_{\mathrm{ML}} + \sum_{n=2}^{6} \left(a_{n,k,\mathrm{ML}} {r_{\mathrm{ML}}}^{-n}\right) \tag{5}$$

Further details on the calculation of the energy and the gradient have been described elsewhere.[32,55] Alternative AOM approaches have also been developed recently and applied with promising results.[39−42]

The empirical term estimating the additional interelectronic repulsion due to electron pairing in low-spin models is defined for each metal center by a polynomial function of the metal−ligand bond lengths r_{ML_i} according to eq 6,

$$E_{\mathrm{pair}} = w \sum_{i}^{\text{ligands}} \left[p_{0,\mathrm{ML}_i} + p_{1,\mathrm{ML}_i} r_{\mathrm{ML}_i} + \sum_{n=2}^{6} \left(a_{n,\mathrm{ML}_i} {p_{\mathrm{ML}_i}}^{-n}\right)\right] \tag{6}$$

in which the p_{n,ML_i} are LFMM parameters and w is a weighting factor (w = 1 for low-spin metal centers and w = 0 for high-spin metal centers). Treatment of intermediate-spin states is less systematic, as various weighting factors can be used, and has not been implemented in this version.

For the metal−ligand bond stretching terms, either harmonic (eq 7) or Morse-style (eq 8) functional forms can be chosen, in which r_{ML_i} is the metal−ligand bond length and $r^{\mathrm{eq}}_{\mathrm{ML}_i}$, k_{ML_i}, D_{ML_i}, and α_{ML_i} are the LFMM parameters. Also for the 1−3 ligand−ligand interactions two functional forms can be used in the LFMM model: either a Lennard-Jones-style potential (eq 9) or a purely repulsive potential (eq 10), in which $r_{\mathrm{L}_i\mathrm{L}_j}$ is the distance between the coordinating atoms of different ligands, m and n are fixed LFMM parameters, and $A_{\mathrm{L}_i\mathrm{L}_j}$, $B_{\mathrm{L}_i\mathrm{L}_j}$, and $C_{\mathrm{L}_i\mathrm{L}_j}$ are LFMM parameters or, for ligand pairs of different types, the geometric means of the LFMM parameters. It should be noted that for pairs involving very different kinds of ligands, the geometric mean might not be suitable,[56] and the implementation of further combination rules may be needed. Moreover, while the standard Lennard-Jones functional form can be applied for L−L pairs, dedicated parameters must be used since the standard van der Waals parameters are in general not suitable for 1−3 nonbonded interactions.[57]

$$E_{\mathrm{ML,harm}} = \sum_{i}^{\text{harm. ligands}} \frac{1}{2} k_{\mathrm{ML}_i} \left(r_{\mathrm{ML}_i} - r^{\mathrm{eq}}_{\mathrm{ML}_i}\right)^2 \tag{7}$$

DOI: 10.1021/acs.jcim.5b00098
J. Chem. Inf. Model. 2015, 55, 1282−1290

$$E_{\mathrm{ML,Morse}} = \sum_{i}^{\substack{\mathrm{Morse}\\ \mathrm{ligands}}} \{D_{\mathrm{ML}_i}[1 - \mathrm{e}^{-\alpha_{\mathrm{ML}_i}(r_{\mathrm{ML}_i} - r_{\mathrm{ML}_i}^{\mathrm{eq}})}]^2 - D_{\mathrm{ML}_i}\} \tag{8}$$

$$E_{\mathrm{L}_i\mathrm{L}_j\mathrm{vdW}} = \sum_{i>j} \left(\frac{A_{\mathrm{L}_i\mathrm{L}_j}}{r_{\mathrm{L}_i\mathrm{L}_j}^{\ m}} - \frac{B_{\mathrm{L}_i\mathrm{L}_j}}{r_{\mathrm{L}_i\mathrm{L}_j}^{\ 6}} \right) \tag{9}$$

$$E_{\mathrm{L}_i\mathrm{L}_j\mathrm{rep}} = \sum_{i>j} C_{\mathrm{L}_i\mathrm{L}_j} r_{\mathrm{L}_i\mathrm{L}_j}^{\ -n} \tag{10}$$

Finally, some of the existing LFMM parametrizations[58,59] include restraints to alter the potential energy profiles of metal−ligand bond stretches:

$$E_{\mathrm{ML}_i,\mathrm{Morse}}^{\mathrm{short}} = E_{\mathrm{ML}_i,\mathrm{Morse}} + w[(r_{\mathrm{ML}_i}^{\mathrm{eq}} - R_{\mathrm{short}})^2 - r_{\mathrm{ML}_i}^{\ 2}]^3 \tag{11}$$

$$\text{when} \quad (r_{\mathrm{ML}_i}^{\mathrm{eq}} - R_{\mathrm{short}})^2 - r_{\mathrm{ML}_i}^{\ 2} > 0 \tag{12}$$

and

$$E_{\mathrm{ML}_i,\mathrm{Morse}}^{\mathrm{long}} = E_{\mathrm{ML}_i,\mathrm{Morse}} + w[r_{\mathrm{ML}_i}^{\ 2} - (r_{\mathrm{ML}_i}^{\mathrm{eq}} + R_{\mathrm{long}})^2]^3 \tag{13}$$

$$\text{when} \quad r_{\mathrm{ML}_i}^{\ 2} - (r_{\mathrm{ML}_i}^{\mathrm{eq}} + R_{\mathrm{long}})^2 > 0 \tag{14}$$

where the parameters R_{short}, R_{long}, and the weight w apply to all metal−ligand pairs. The restraints define an additional (always positive) potential energy contribution that disfavors metal−ligand bond lengths outside the range defined by $r_{\mathrm{ML}_i}^{\mathrm{eq}} - R_{\mathrm{short}}$ and $r_{\mathrm{ML}_i}^{\mathrm{eq}} + R_{\mathrm{long}}$, thus avoiding ligand dissociation and the unphysical collapse of a ligand onto the metal atom, which may, depending on the LFMM parameters, be favored by the LFSE term.

IMPLEMENTATION

Tinker provides a set of programs for molecular mechanics and dynamics calculations together with various tools and utilities for modeling of molecules as well as biopolymers.[60] The source code is organized into programs, which are directly called by the user, and a modular structure of routines, which are called by programs to perform specific tasks, i.e., assignment of force constants to various interactions and calculation of the contributions to the energy and derivatives (Figure 2). To make the implementation of LFMM in Tinker as user-friendly as possible without requiring a graphical user interface, all of the new routines are interfaced to existing Tinker programs, and a set of new keywords (see the documentation in distribution folder)[61] allows for detailed control over the settings without requiring cumbersome preparation of input files for the AOM calculations. In fact, to perform LFMM-based calculations with default settings for the kind of calculation to be performed (e.g., single-point calculation, geometry optimization, or MD simulation), the user executes the corresponding Tinker program (e.g., *analyze*, *minimize*, *optimize*, or *dynamic*) and provides a standard keyword file with additional information specifying the atom(s) that should be treated as LFMM metal center(s), the number of d electrons, and the spin state of each metal center. Further options are available depending on the specific application.

To enable Tinker to do LFMM calculations, the ligand field stabilization energy routine (*clfse* in Figure 2), which performs the AOM calculations and was originally written as part of DOMMINO,[29,32] has been interfaced with the Tinker routines for calculation of the energy and energy derivatives (i.e., the routines *energy*, *gradient*, and *hessian*). The *clfse* routine calculates the LFSE and the analytical first derivatives for a single metal center at a time since each metal center is treated independently from the others. Analytical second derivatives are not available, and thus, the finite-difference approximation is adopted for numerical differentiation of the analytical first derivatives. In contrast to the LFSE term, the routines providing energy and analytical derivatives for the remaining LFMM contributions, i.e., the empirical electron pairing energy, the M−L bond stretches, and the ligand−ligand interactions, were added directly to the Tinker source code (Figure 2). The same applies to routines for assignment and handling of LFMM-related parameters (*klfmm* in Figure 2).

Next, to prevent the metal-related terms, such as L−M−L bending and M−L bond stretching, to be included twice and to ensure compatibility with existing LFMM parametrizations, the classical MM contributions of the standard force fields implemented in Tinker either had to be turned off or adapted for these interactions. To annihilate standard bending and stretching terms involving the metal atoms, force constants equal to zero are imposed. To this end, instead of acting on the force field parameters provided as input (i.e., the parameter file), routines have been added to identify and overwrite the internal values of the specific force constants that are otherwise assigned according to the standard force field in use for the organic portion of the system (i.e., AMBER, MMFF94).

Collinear L−M−L triads are common in transition-metal complexes, and since such an arrangement of atoms prevents the definition of dihedral angles involving these triads, M−L torsional twist should not always be considered by default. Nevertheless, for specific applications not suffering from collinear L−M−L triads, a nonzero potential for the M−L torsional twist may be required. Therefore, the capability to calculate such potentials was maintained, and zeroing of the force constants in the parameter file was chosen as a means to ignore M−L torsional twist in LFMM calculations.

In the LFMM method, the organic portion of the transition-metal complex should be handled by a standard force field such as MMFF94 or AMBER. Although this is certainly true for most of the applications, the optimization of LFMM force fields has shown that better results can be achieved through adaptation of a few parameters also in the "organic" force field, use of constraints, and even alterations of the canonical functional forms describing the potential energy of specific contributions.[57,59,62] The latter has in particular involved using polynomial functional forms with independent coefficients k', k'', and k''' for bond stretching according to eq 15, where r_{ij} is the interatomic distance and r_{ij}^{eq} is the equilibrium value, and bending terms following eq 16, where ϕ_{ijk} is the bond angle identified by atoms i, j, and k and ϕ_{ijk}^{eq} is the equilibrium value:

$$E_{ij,\mathrm{str}} = k_{\mathrm{b}}'\delta_{ij}^{\ 2} + k_{\mathrm{b}}''\delta_{ij}^{\ 3} + k_{\mathrm{b}}'''\delta_{ij}^{\ 4} \tag{15}$$

$$E_{ijk}^{\mathrm{ang}} = k_{\mathrm{a}}'\theta_{ijk}^{\ 2} + k_{\mathrm{a}}''\theta_{ijk}^{\ 3} + k_{\mathrm{a}}'''\theta_{ijk}^{\ 4} \tag{16}$$

in which $\delta_{ij} = r_{ij} - r_{ij}^{\mathrm{eq}}$ and $\theta_{ijk} = \phi_{ijk} - \phi_{ijk}^{\mathrm{eq}}$.

While many force fields use the simple harmonic approximation (i.e., truncating eqs 15 and 16 after the quadratic terms), a more general polynomial form based on independent coefficients is adopted in some cases, for instance

DOI: 10.1021/acs.jcim.5b00098
J. Chem. Inf. Model. 2015, 55, 1282−1290

in CFF91/93.[63] Other popular force fields, such as MMFF94,[4] MM2/3/4,[3,64] and AMOEBA,[65] are based on polynomial functions (eq 17) in which all of the coefficients are related to the lowest-order one by means of fixed factors (c_b and q_b in eq 17) that are kept equal for all interactions of the same term (i.e., different bond stretches use different force constants k'_b but identical factors c_b and q_b):

$$E_{ij}^{str} = k'_b\delta_{ij}^2(1 + c_b\delta_{ij} + q_b\delta_{ij}^2) \quad (17)$$

All of the force fields currently deployed in Tinker stick to the polynomial form of eq 17 or the closely related harmonic form in which $c_b = q_b = 0$. Therefore, to provide the flexibility that the LFMM parameter sets require and to ensure backward compatibility, we extended the list of MM functional forms for bond stretching and angle bending implemented in Tinker by adding the independent-coefficients polynomial forms shown in eqs 15 and 16. In addition, for MMFF-style force fields the torsional potential was extended to include up to the 6-fold term. It should be stressed, however, that while the abundance of independent parameters provided by these functional forms allows for ample flexibility, the side effect is more challenging parametrization work if balanced, transferable, and robust force fields are to be developed.[66]

All of the additional energy terms and functional forms implemented for LFMM are based on empirical parameters collected in the parameter file using Tinker-style formatting. In particular, Tinker *atom class numbers* are used to report the LFMM parameters in Tinker's parameter file. Automatic assignment of atom types is not implemented in Tinker. Therefore, the atom type of the metal atom must be set explicitly in the input file along with those of all of the other atoms of the system.

Finally, the current implementation of LFMM in Tinker has been validated against numerical results obtained using DommiMOE (see the Supporting Information for details) and is applicable to chemical systems containing one or more monometallic complexes (one metal atom per LFMM center), each with up to 12 monohapto ligands surrounding the single metal atom. Support for treatment of intermediate-spin states and π complexes has not yet been implemented, and this will be the subject of future work since LFMM has also proved capable of describing complexes with π-bonded ligands.[28,31] We are currently exploring with the Tinker developers how best to distribute the Tinker-LFMM code to the wider academic community.[61]

■ ILLUSTRATIVE EXAMPLES

The LFSE term is calculated from the formal occupation of the d orbitals of the metal (eq 3). This, combined with the electron pairing energy, makes the LFMM method capable of modeling high- and low-spin states using a single set of empirical parameters. To illustrate, we consider the simple complex hexaammineiron(II), $[Fe(NH_3)_6]^{2+}$. While this complex is high-spin in the solid state, species hosting the FeN_6 motif have shown spin-crossover properties that may open up a range of technological applications.[67−69] The possibility of modeling, at low computational cost, both high- and low-spin states of species such as hexaammineiron(II) enables the study and design of FeN_6 species for potential applications, and LFMM force fields have been developed specifically for this purpose.[58,59]

Optimized geometries for the high-spin (HS, $^5T_{2g}$) and low-spin (LS, $^1A_{1g}$) states of hexaammineiron(II) were obtained in searches for the global minimum using the program *monte* (consisting of a Monte Carlo minimization algorithm) of the LFMM-integrated Tinker package.[60] In this example, we made use of the LFMM force field developed by Deeth and co-workers (labeled "R5S7" in ref 59), which is optimized to reproduce both geometries and energy differences (Δ) between LS and HS states as calculated at the DFT level for this type of compound. Good agreement between DFT (data from ref 59) and LFMM is found with respect to both the Fe−N bond length (HS_{LFMM}, 2.32 Å; HS_{DFT}, 2.20 Å; LS_{LFMM}, 2.04 Å; LS_{DFT}, 2.02 Å) and the relative energies of the optimized geometries (Δ_{LFMM} = 6.08 kcal/mol; Δ_{DFT} = 6.76 kcal/mol). The observed deviation in the bond length for the HS state is reproduced also with the original implementation of LFMM (in DommiMOE) and arises because the force field parameters overall are more accurate in reproducing the HS−LS energy gap across a variety of molecules than the geometry of single compound.[59] The empirical electron pairing energy is here taken into account only for the LS model, which, combined with the change in LFSE due to the different d-orbital occupation, determines the shorter Fe−N bond length of the LS geometry.

The crucial role of the LFSE term and its balance with the other contributions affecting the bond length is illustrated by calculations on the copper(II) complexes $[Cu(NH_3)_m]^{2+}$ (m = 4, 5, 6), for which we made use of the force field developed in ref 57. With a d^9 configuration, the octahedral hexaammine complex has partially filled and degenerate e_g orbitals that constitute a textbook example of the Jahn−Teller effect.[70] The octahedral geometry of $[Cu(NH_3)_6]^{2+}$ is unstable with respect to a tetragonal perturbation that removes the orbital degeneracy and lowers the electronic energy.[57,71] The resulting low-energy geometry is characterized by two elongated trans-related Cu−N bonds, conventionally labeled as the axial positions, and four shortened equatorial Cu−N bonds. Reproducing such a geometry with the bond stretching potentials of standard force fields alone would require different parameters for compressed and elongated bonds.[72,73] In contrast, the LFSE term adopted by the LFMM approach allows the system to be modeled using a single set of parameters for all six ligands.[57,71,74] To illustrate, the geometry of $[Cu(NH_3)_6]^{2+}$ was first modeled using a modified potential *not* including the LFSE term.[75] The lowest-energy geometry obtained using the *monte* program is that of a perfectly octahedral system with six equally long Cu−N bonds (2.24 Å). The bond length is the result of compromise between the LFMM M−L stretching and L−L repulsion terms (blue and red, respectively, in Figure 3, A1), both of which are spherically symmetric around each of the interacting atoms and unable to introduce the anisotropy caused by the Jahn−Teller effect.

The calculation of the LFSE contribution to the gradient (obtained via Tinker's *analyze* program) in the geometry optimized with an LFSE-free potential shows how the anisotropy is introduced by the LFSE term as forces compressing the equatorial metal−ligand bonds and elongating the axial ones (Figure 3, B1). Consequently, the lowest-energy geometry for the potential including all of the contributions is a tetragonal geometry with the qualitatively correct difference between the axial and equatorial Cu−N bond distances (2.37 and 2.06 Å, respectively). The decomposition of the force components in the latter geometry (Figure 3, C1) shows that the negligible total force on each of the N atoms (root-mean-

DOI: 10.1021/acs.jcim.5b00098
J. Chem. Inf. Model. 2015, 55, 1282−1290

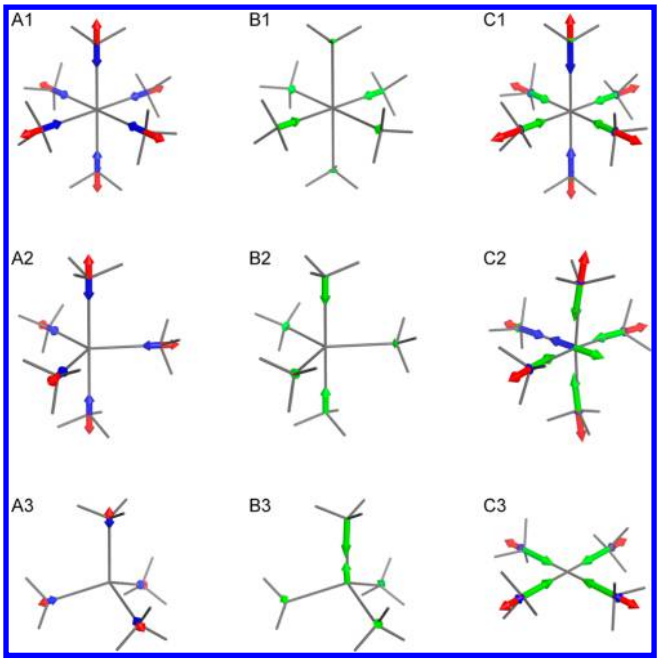

Figure 3. Representation of force components acting on copper and nitrogen atoms of $[Cu(NH_3)_m]^{2+}$ (m = 4, 5, 6) . For each coordination number, the three pictures represent the balance between M−L stretching (blue) and L−L repulsion (red) forces in the minimum-energy geometry optimized with an LFSE-free potential (A1, A2, A3); the neglected LFSE forces (green) for the same geometry depicted in the leftmost column (B1, B2, B3); and the balance of M−L stretching (blue), L−L repulsion (red), and LFSE (green) force components at the lowest-energy geometry optimized with all of the potential energy contributions, including the LFSE term (C1, C2, C3). For clarity, negligible forces are not shown.

square gradient < 0.001 kcal/mol) is the result of the balance between different kinds of contributions for the axial and the equatorial ligands. For the axial ligands, the balance involves mainly the M−L stretching and L−L repulsive components with a minor yet significant LFSE contribution that still pushes the metal and ligand apart (note that the head of the green vector in Figure 3, C1 is partially hidden by the other, stronger contributions). On the contrary, the LFSE force component for the equatorial ligands is strong and has the opposite direction (i.e., shortening the metal−ligand bond), and thus, the balance between the LFSE component and other contributions is obtained at a shorter bond length than for the axial ligands.

A similar analysis was performed for the penta- and tetracoordinate complexes of copper(II), i.e., for $[Cu(NH_3)_m]^{2+}$ with m = 4 and 5, using in both cases the same force field.[57] In contrast to the hexacoordinate complex, where the distortion introduced by the LFSE affects only the metal−ligand bond lengths, the entire coordination geometries of both $[Cu(NH_3)_4]^{2+}$ and $[Cu(NH_3)_5]^{2+}$ change upon introduction of the LFSE term. In fact, optimizing the geometry without this contribution returns coordination geometries that minimize the ligand−ligand repulsion, namely, a trigonal bipyramid for m = 5 (Figure 3, A2) and a tetrahedron for m = 4 (Figure 3, A3).[32] Just as for the hexacoordinate case (A1), the Cu−N bond lengths are determined by a compromise between the L−L repulsion and M−L stretching terms and are 2.21 Å (axial) and 2.17 Å (equatorial) in the pentacoordinate complex (A2) and 2.12 Å in the tetrahedron (A3).

The LFSE contribution to the gradient in the pentacoordinate complex calculated on the geometry optimized with the LFSE-free potential (Figure 3, B2) implies compression of all of the Cu−N bonds. Instead, in agreement with experiment,[57] the global minimum on the energy surface of the complete potential including the LFSE term, obtained with the program *monte*, is a square-pyramidal geometry (Figure 3, C2) with short equatorial bonds (2.02 Å) and an elongated axial bond (2.35 Å). Similarly, the LFSE term neglected in the calculation on the tetracoordinate complex (Figure 3, B3) describes the contraction of one metal−ligand bond and the apparent movement of the remaining ligands toward a trigonal-pyramidal geometry. However, the lowest-energy geometry in the fully defined potential, including the LFSE term, is found to be square-planar (Figure 3, C3). This structure, consistent with experimental observation,[57] is characterized by short Cu−N bonds (1.98 Å) resulting from the strong LFSE contributions, which compensate for the combination of the L−L repulsion and M−L Morse-like stretching terms, the latter being repulsive at such short distances.

While the last two examples demonstrate that the LFSE contribution affects not only the bond lengths but also the overall coordination geometry, they also show that inclusion of the LFSE term may lead to multiple local minima even for relatively small transition-metal complexes. In fact, reoptimization of geometry A2 in Figure 3 including the LFSE term, using either the *minimize* or *optimize* program, results in an axially compressed trigonal-bipyramidal geometry, the expected result of the force components depicted in geometry B2 in Figure 3 (also see structure D2 in the Supporting Information). Thus, in this case the global minimum is reached only when a basin-hopping method such as that of the program *monte* is used.

The LFMM potential may also form the basis for MD simulations (termed the LFMD method). For example, single-molecule LFMD trajectories have been reported to account for the dynamic behavior of FeN_6 spin-crossover compounds.[58] The fluctuations of the Fe(II) HS−LS relative stability as a function of simulation temperature have been found to follow, qualitatively, the temperature behavior of the experimentally observed spin-state transition.[76] Here we used this spin transition as a test case to demonstrate the applicability of the Tinker-LFMM implementation to MD simulations. A range of LFMD trajectories for the FeN_6 spin-crossover system of ref 58 (depicted in Figure S2 in the Supporting Information) were obtained using Tinker and, for comparison, DommiMOE (the software used in ref 58). The use of two different programs (the algorithms and settings of which are mutually impossible to reproduce exactly) and the stochastic nature of initial MD velocities imply that MD trajectories obtained with one program cannot readily be duplicated in the second. Also, each pair of LS and HS trajectories should not be expected to reproduce an experimentally observed spin transition. Averages obtained for sets of independent trajectories, however, can tell something about the relative stabilities of the two spin states and the location of a spin transition.

Gratifyingly, the trends in the relative spin state stability obtained using DommiMOE are reproduced with the Tinker implementation (see Tables S1−S5 in the Supporting Information). Specifically, whereas the average potential energy of the LS state at 220 K is almost always lower than that of the HS state, the LS and HS potential energies are more similar at 360 K, with the HS state being preferred in some trajectories. Keeping in mind the above-mentioned stochastic nature of MD

DOI: 10.1021/acs.jcim.5b00098
J. Chem. Inf. Model. 2015, 55, 1282−1290

results, this trend qualitatively reflects the experimental observation of a spin transition between the two temperatures,[76] as first noted for analogous MD trajectories in ref 58. Although many of the energy gaps between the LS and HS states in Tables S1−S5 are very narrow and do not firmly locate the spin transition between the two temperatures, and a more quantitative reproduction of the experimentally observed spin inversion probably would require improvement of the force field, our work demonstrates that the Tinker-LFMM implementation may be used to study both the static and dynamic properties of transition-metal compounds.

CONCLUSIONS

The ligand field molecular mechanics (LFMM) method has been implemented in the popular and readily available molecular modeling package Tinker. The LFMM method requires specific potential energy terms and functional forms that are not available in most common molecular modeling tools, and expanding the capabilities of Tinker has been necessary in order to integrate LFMM. The resulting LFMM-capable and easily available molecular modeling software allows for a broad range of applications of LFMM and should also stimulate further developments of parameter sets and of the LFMM method itself.

ASSOCIATED CONTENT

Supporting Information

Molecular structures, force field parameters, and a summary of the validation study. The Supporting Information is available free of charge on the ACS Publications website at DOI: 10.1021/acs.jcim.5b00098.

AUTHOR INFORMATION

Corresponding Authors

*E-mail: R.J.Deeth@warwick.ac.uk.
*E-mail: vidar.jensen@kj.uib.no.

Notes

The authors declare no competing financial interest.

ACKNOWLEDGMENTS

The Research Council of Norway (RCN) is acknowledged for financial support via the eVITA program (Grant 205273) and for CPU (Grant NN2506K) and storage (Grant NS2506K) resources. Network support by COST Action CM1305 (eCOSTBIO) is also gratefully acknowledged. R.J.D. acknowledges the generous support of Chemical Computing Group.

REFERENCES

(1) Boeyens, J. C. A.; Comba, P. Molecular Mechanics: Theoretical Basis, Rules, Scope and Limits. *Coord. Chem. Rev.* **2001**, *212*, 3−10.
(2) Comba, P.; Kerscher, M. Computation of Structures and Properties of Transition Metal Compounds. *Coord. Chem. Rev.* **2009**, *253*, 564−574.
(3) Allinger, N. L.; Yuh, Y. H.; Lii, J. H. Molecular Mechanics. The MM3 Force Field for Hydrocarbons. 1. *J. Am. Chem. Soc.* **1989**, *111*, 8551−8566.
(4) Halgren, T. A. Merck Molecular Force Field. I. Basis, Form, Scope, Parameterization, and Performance of MMFF94. *J. Comput. Chem.* **1996**, *17*, 490−519.
(5) Cornell, W. D.; Cieplak, P.; Bayly, C. I.; Gould, I. R.; Merz, K. M., Jr.; Ferguson, D. M.; Spellmeyer, D. C.; Fox, T.; Caldwell, J. W.; Kollman, P. A. A Second Generation Force Field for the Simulation of Proteins, Nucleic Acids, and Organic Molecules. *J. Am. Chem. Soc.* **1995**, *117*, 5179−5197.
(6) Comba, P.; Remenyi, R. Inorganic and Bioinorganic Molecular Mechanics Modeling—The Problem of the Force Field Parameterization. *Coord. Chem. Rev.* **2003**, *238*−*239*, 9−20.
(7) Bernhardt, P. V.; Comba, P. Molecular Mechanics Calculations of Transition Metal Complexes. *Inorg. Chem.* **1992**, *31*, 2638−2644.
(8) Landis, C. R.; Root, D. M.; Cleveland, T. Molecular Mechanics Force Fields for Modeling Inorganic and Organometallic Compounds. *Rev. Comput. Chem.* **1995**, *6*, 73−148.
(9) Norrby, P.-O.; Brandt, P. Deriving Force Field Parameters for Coordination Complexes. *Coord. Chem. Rev.* **2001**, *212*, 79−109.
(10) Hay, B. P. Methods for Molecular Mechanics Modeling of Coordination Compounds. *Coord. Chem. Rev.* **1993**, *126*, 177−236.
(11) Hu, L.; Ryde, U. Comparison of Methods To Obtain Force-Field Parameters for Metal Sites. *J. Chem. Theory Comput.* **2011**, *7*, 2452−2463.
(12) Norrby, P.-O.; Liljefors, T. Automated Molecular Mechanics Parameterization with Simultaneous Utilization of Experimental and Quantum Mechanical Data. *J. Comput. Chem.* **1998**, *19*, 1146−1166.
(13) Reichert, D. E.; Norrby, P.-O.; Welch, M. J. Molecular Modeling of Bifunctional Chelate Peptide Conjugates. 1. Copper and Indium Parameters for the AMBER Force Field. *Inorg. Chem.* **2001**, *40*, 5223−5230.
(14) Hagelin, H.; Svensson, M.; Åkermark, B.; Norrby, P.-O. Molecular Mechanics (MM3*) Force Field Parameters for Calculations on Palladium Olefin Complexes with Phosphorus Ligands. *Organometallics* **1999**, *18*, 4574−4583.
(15) Rappé, A. K.; Casewit, C. J.; Colwell, K. S.; Goddard, W. A., III; Skiff, W. M. UFF, a Full Periodic Table Force Field for Molecular Mechanics and Molecular Dynamics Simulations. *J. Am. Chem. Soc.* **1992**, *114*, 10024−10035.
(16) Addicoat, M. A.; Vankova, N.; Akter, I. F.; Heine, T. Extension of the Universal Force Field to Metal−Organic Frameworks. *J. Chem. Theory Comput.* **2014**, *10*, 880−891.
(17) Shi, S.; Yan, L.; Yang, Y.; Fisher-Shaulsky, J.; Thacher, T. An Extensible and Systematic Force Field, ESFF, for Molecular Modeling of Organic, Inorganic, and Organometallic Systems. *J. Comput. Chem.* **2003**, *24*, 1059−1076.
(18) Allured, V. S.; Kelly, C. M.; Landis, C. R. SHAPES Empirical Force Field: New Treatment of Angular Potentials and Its Application to Square-Planar Transition-Metal Complexes. *J. Am. Chem. Soc.* **1991**, *113*, 1−12.
(19) Comba, P.; Hambley, T. W.; Martin, B. *Molecular Modeling of Inorganic Compounds*; Wiley-VCH: Weinheim, Germany, 2009.
(20) Root, D. M.; Landis, C. R.; Cleveland, T. Valence Bond Concepts Applied to the Molecular Mechanics Description of Molecular Shapes. 1. Application to Nonhypervalent Molecules of the P-Block. *J. Am. Chem. Soc.* **1993**, *115*, 4201−4209.
(21) Landis, C. R.; Cleveland, T.; Firman, T. K. Valence Bond Concepts Applied to the Molecular Mechanics Description of Molecular Shapes. 3. Applications to Transition Metal Alkyls and Hydrides. *J. Am. Chem. Soc.* **1998**, *120*, 2641−2649.
(22) Firman, T. K.; Landis, C. R. Valence Bond Concepts Applied to the Molecular Mechanics Description of Molecular Shapes. 4. Transition Metals with π-Bonds. *J. Am. Chem. Soc.* **2001**, *123*, 11728−11742.
(23) Schmid, M. H.; Ward, T. R.; Meuwly, M. Toward a Broadly Applicable Force Field for d^6-Piano Stool Complexes. *J. Chem. Theory Comput.* **2013**, *9*, 2313−2323.
(24) Tubert-Brohman, I.; Schmid, M.; Meuwly, M. Molecular Mechanics Force Field for Octahedral Organometallic Compounds with Inclusion of the Trans Influence. *J. Chem. Theory Comput.* **2009**, *5*, 530−539.
(25) Deeth, R. J. The Ligand Field Molecular Mechanics Model and the Stereoelectronic Effects of d and s Electrons. *Coord. Chem. Rev.* **2001**, *212*, 11−34.
(26) Ćendić, M.; Matović, Z. D.; Deeth, R. J. Molecular Modeling for Cu(II)−Aminopolycarboxylate Complexes: Structures, Conforma-

DOI: 10.1021/acs.jcim.5b00098
J. Chem. Inf. Model. 2015, 55, 1282−1290

tional Energies, and Ligand Binding Affinities. *J. Comput. Chem.* **2013**, *34*, 2687−2696.
(27) Tai, H.-C.; Brodbeck, R.; Kasparkova, J.; Farrer, N. J.; Brabec, V.; Sadler, P. J.; Deeth, R. J. Combined Theoretical and Computational Study of Interstrand DNA Guanine−Guanine Cross-Linking by *trans*-[Pt(pyridine)$_2$] Derived from the Photoactivated Prodrug *trans,trans,trans*-[Pt(N$_3$)$_2$(OH)$_2$(pyridine)$_2$]. *Inorg. Chem.* **2012**, *51*, 6830−6841.
(28) Brodbeck, R.; Deeth, R. J. Extending Ligand Field Molecular Mechanics to Modelling Organometallic π-Bonded Systems: Applications to Ruthenium−Arenes. *Dalton Trans.* **2011**, *40*, 11147−11155.
(29) Burton, V. J.; Deeth, R. J. Molecular Modelling for Copper(II) Centres. *J. Chem. Soc., Chem. Commun.* **1995**, 573−574.
(30) Anastasi, A. E.; Deeth, R. J. Capturing the Trans Influence in Low-Spin d^8 Square-Planar Platinum(II) Systems Using Molecular Mechanics. *J. Chem. Theory Comput.* **2009**, *5*, 2339−2352.
(31) Diedrich, C.; Deeth, R. J. On the Performance of Ligand Field Molecular Mechanics for Model Complexes Containing the Peroxido-Bridged $[Cu_2O_2]_2^+$ Center. *Inorg. Chem.* **2008**, *47*, 2494−2506.
(32) Burton, V. J.; Deeth, R. J.; Kemp, C. M.; Gilbert, P. J. Molecular Mechanics for Coordination Complexes: The Impact of Adding d-Electron Stabilization Energies. *J. Am. Chem. Soc.* **1995**, *117*, 8407−8415.
(33) Deeth, R. J.; Anastasi, A.; Diedrich, C.; Randell, K. Molecular Modelling for Transition Metal Complexes: Dealing with d-Electron Effects. *Coord. Chem. Rev.* **2009**, *253*, 795−816.
(34) Solomon, E. I.; Scott, R. A.; King, R. B. *Computational Inorganic and Bioinorganic Chemistry*; John Wiley & Sons: Hoboken, NJ, 2013.
(35) Molecular Mechanics in Bioinorganic Chemistry. In *Encyclopedia of Inorganic and Bioinorganic Chemistry* [Online]; John Wiley & Sons, 2011. http://onlinelibrary.wiley.com/doi/10.1002/9781119951438.eibc0403/full (accessed May 5, 2015).
(36) Deeth, R. J.; Fey, N.; Williams-Hubbard, B. DommiMOE: An Implementation of Ligand Field Molecular Mechanics in the Molecular Operating Environment. *J. Comput. Chem.* **2005**, *26*, 123−130.
(37) Chemical Computing Group Inc. Molecular Operating Environment (MOE), version 2011.10. https://www.chemcomp.com/MOE-Molecular_Operating_Environment.htm (accessed March 2014).
(38) Smith, W.; Yong, C. W.; Rodger, P. M. DL_POLY: Application to Molecular Simulation. *Mol. Simul.* **2002**, *28*, 385−471.
(39) Carlsson, A. E.; Zapata, S. The Functional Form of Angular Forces around Transition Metal Ions in Biomolecules. *Biophys. J.* **2001**, *81*, 1−10.
(40) Piquemal, J.-P.; Williams-Hubbard, B.; Fey, N.; Deeth, R. J.; Gresh, N.; Giessner-Prettre, C. Inclusion of the Ligand Field Contribution in a Polarizable Molecular Mechanics: SIBFA-LF. *J. Comput. Chem.* **2003**, *24*, 1963−1970.
(41) Woodley, S. M.; Battle, P. D.; Catlow, C. R. A.; Gale, J. D. Development of a New Interatomic Potential for the Modeling of Ligand Field Effects. *J. Phys. Chem. B* **2001**, *105*, 6824−6830.
(42) Xiang, J. Y.; Ponder, J. W. An Angular Overlap Model for Cu(II) Ion in the AMOEBA Polarizable Force Field. *J. Chem. Theory Comput.* **2014**, *10*, 298−311.
(43) Zimmer, M. Are Classical Molecular Mechanics Calculations Still Useful in Bioinorganic Simulations? *Coord. Chem. Rev.* **2009**, *253*, 817−826.
(44) Ponder, J. W. TINKER, version 6.3. http://dasher.wustl.edu/tinker/ (accessed March 2014).
(45) Schäffer, C. E.; Jørgensen, C. K. The Angular Overlap Model, an Attempt To Revive the Ligand Field Approaches. *Mol. Phys.* **1965**, *9*, 401−412.
(46) Gerloch, M.; Harding, J. H.; Woolley, R. G. The Context and Application of Ligand Field Theory. *Struct. Bonding* **1981**, *46*, 1−46.
(47) Schönherr, T.; Atanasov, M.; Adamsky, H. Angular Overlap Model. In *Comprehensive Coordination Chemistry II*; McCleverty, J. A., Meyer, T. J., Eds.; Pergamon Press: Oxford, U.K., 2003; Vol. 2, pp 443−455.
(48) Bernhardt, P. V.; Comba, P. Prediction and Interpretation of Electronic Spectra of Transition Metal Complexes via the Combination of Molecular Mechanics and Angular Overlap Model Calculations. *Inorg. Chem.* **1993**, *32*, 2798−2803.
(49) Comba, P.; Hambley, T. W.; Hitchman, M. A.; Stratemeier, H. Interpretation of Electronic and EPR Spectra of Copper(II) Amine Complexes: A Test of the MM-AOM Method. *Inorg. Chem.* **1995**, *34*, 3903−3911.
(50) Comba, P.; Hilfenhaus, P.; Nuber, B. The Structure of an Isomeric Pair of a (Tetraamine)copper(II) Compound in the Solid State and in Solution. *Helv. Chim. Acta* **1997**, *80*, 1831−1842.
(51) Börzel, H.; Comba, P.; Pritzkow, H.; Sickmüller, A. F. Preparation, Structure, and Electronic Properties of a Low-Spin Iron(II) Hexaamine Compound. *Inorg. Chem.* **1998**, *37*, 3853−3857.
(52) Hoggard, P. E. Angular Overlap Model Parameters. *Struct. Bonding* **2004**, *106*, 37−57.
(53) Bridgeman, A. J.; Gerloch, M. The Interpretation of Ligand Field Parameters. *Prog. Inorg. Chem.* **1996**, *45*, 179−281.
(54) Comba, P. Strains and Stresses in Coordination Compounds. *Coord. Chem. Rev.* **1999**, *182*, 343−371.
(55) Deeth, R. J.; Foulis, D. L. Analytical Derivatives, π Bonding and d−s Mixing in the Ligand Field Molecular Mechanics Method. *Phys. Chem. Chem. Phys.* **2002**, *4*, 4292−4297.
(56) Waldman, M.; Hagler, A. T. New Combining Rules for Rare Gas van der Waals Parameters. *J. Comput. Chem.* **1993**, *14*, 1077−1084.
(57) Deeth, R. J.; Hearnshaw, L. J. A. Molecular Modelling for Coordination Compounds: Cu(II)−Amine Complexes. *Dalton Trans.* **2005**, 3638−3645.
(58) Deeth, R. J.; Anastasi, A. E.; Wilcockson, M. J. An In Silico Design Tool for Fe(II) Spin Crossover and Light-Induced Excited Spin State-Trapped Complexes. *J. Am. Chem. Soc.* **2010**, *132*, 6876−6877.
(59) Handley, C. M.; Deeth, R. J. A Multi-Objective Approach to Force Field Optimization: Structures and Spin State Energetics of d^6 Fe(II) Complexes. *J. Chem. Theory Comput.* **2012**, *8*, 194−202.
(60) Tinker Users's Guide and Tutorial. http://dasher.wustl.edu/tinkerwiki/index.php/Main_Page (accessed Dec 10, 2014).
(61) The LFMM code described here will be distributed as part of a coming Tinker release. Information on the distribution of the Tinker-LFMM code will appear on the Tinker website (http://dasher.wustl.edu/tinker/).
(62) Deeth, R. J. General Molecular Mechanics Method for Transition Metal Carboxylates and Its Application to the Multiple Coordination Modes in Mono- and Dinuclear Mn(II) Complexes. *Inorg. Chem.* **2008**, *47*, 6711−6725.
(63) Hwang, M. J.; Stockfisch, T. P.; Hagler, A. T. Derivation of Class II Force Fields. 2. Derivation and Characterization of a Class II Force Field, CFF93, for the Alkyl Functional Group and Alkane Molecules. *J. Am. Chem. Soc.* **1994**, *116*, 2515−2525.
(64) Allinger, N. L.; Chen, K.; Lii, J.-H. An Improved Force Field (MM4) for Saturated Hydrocarbons. *J. Comput. Chem.* **1996**, *17*, 642−668.
(65) Ponder, J. W.; Wu, C.; Ren, P.; Pande, V. S.; Chodera, J. D.; Schnieders, M. J.; Haque, I.; Mobley, D. L.; Lambrecht, D. S.; DiStasio, R. A.; Head-Gordon, M.; Clark, G. N. I.; Johnson, M. E.; Head-Gordon, T. Current Status of the AMOEBA Polarizable Force Field. *J. Phys. Chem. B* **2010**, *114*, 2549−2564.
(66) Huang, J.; Devereux, M.; Hofmann, F.; Meuwly, M. Computational Organometallic Chemistry with Force Fields. In *Computational Organometallic Chemistry*; Wiest, O., Wu, Y., Eds.; Springer: Berlin, 2012; pp 19−46.
(67) Halcrow, M. A. The Spin-States and Spin-Transitions of Mononuclear Iron(II) Complexes of Nitrogen-Donor Ligands. *Polyhedron* **2007**, *26*, 3523−3576.
(68) Gütlich, P.; Hauser, A.; Spiering, H. Thermal and Optical Switching of Iron(II) Complexes. *Angew. Chem., Int. Ed. Engl.* **1994**, *33*, 2024−2054.
(69) Gütlich, P. Spin Crossover—Quo Vadis? *Eur. J. Inorg. Chem.* **2013**, 581−591.

DOI: 10.1021/acs.jcim.5b00098
J. Chem. Inf. Model. 2015, 55, 1282−1290

(70) Halcrow, M. A. Jahn−Teller Distortions in Transition Metal Compounds, and Their Importance in Functional Molecular and Inorganic Materials. *Chem. Soc. Rev.* **2013**, *42*, 1784−1795.
(71) Deeth, R. J.; Hearnshaw, L. J. A. Molecular Modelling of Jahn−Teller Distortions in Cu(II)N_6 Complexes: Elongations, Compressions and the Pathways in between. *Dalton Trans.* **2006**, 1092−1100.
(72) Comba, P.; Zimmer, M. Molecular Mechanics and the Jahn−Teller Effect. *Inorg. Chem.* **1994**, *33*, 5368−5369.
(73) Deeth, R. J.; Hitchman, M. A. Factors Influencing Jahn−Teller Distortions in Six-Coordinate Copper(II) and Low-Spin Nickel(II) Complexes. *Inorg. Chem.* **1986**, *25*, 1225−1233.
(74) Bentz, A.; Comba, P.; Deeth, R. J.; Kerscher, M.; Seibold, B.; Wadepohl, H. Modeling of the Various Minima on the Potential Energy Surface of Bispidine Copper(II) Complexes: A Further Test for Ligand Field Molecular Mechanics. *Inorg. Chem.* **2008**, *47*, 9518−9527.
(75) Force field parameters are available at http://www2.warwick.ac.uk/fac/sci/chemistry/research/deeth/deethgroup/research/lfmm/lfmm_parameters/ (accessed Dec 9, 2014).
(76) Turner, J. W.; Schultz, F. A. Solution Characterization of the Iron(II) Bis(1,4,7-Triazacyclononane) Spin-Equilibrium Reaction. *Inorg. Chem.* **2001**, *40*, 5296−5298.

DOI: 10.1021/acs.jcim.5b00098
J. Chem. Inf. Model. 2015, 55, 1282−1290